NUCLEAR THEORY, Vol. 36 (2017)
eds. M. Gaidarov, N. Minkov, Heron Press, Sofia

Democratic and Nondemocratic Motion of Three Clusters with the Hyperspherical Harmonics

Yu. A. Lashko, **G. F. Filippov**, **V. S. Vasilevsky**

Bogolyubov Institute for Theoretical Physics, Nat. Acad. of Sci. of Ukraine,
14b, Metrolohichna Str., Kyiv 03143, Ukraine

Abstract. We consider a set of three-cluster systems (^{4}He, ^{7}Li, ^{7}Be, ^{8}Be, ^{10}Be) within a microscopic model which involves the hyperspherical harmonics to represent intercluster motion. We selected such three-cluster systems which have at least one binary channel. Our aim is to study whether the hyperspherical harmonics are able and under what conditions to describe two-body channel(s) (nondemocratic motion) or they are suitable for describing three-cluster continuum only (democratic motion). The main result of the present investigations is that it is possible to see the evidence of two-cluster structure in the three-cluster wave function of a pseudo-bound state yet with a rather restricted set of the hyperspherical harmonics and hyperradial excitations as well.

1 Introduction

The hyperspherical harmonics (HH) method is a powerful tool for solving many-body problems in different branches of quantum physics, namely atomic, molecular and nuclear physics. In the orthodox realization of the method, a many-body problem is reduced to a finite or an infinite set of coupled channel problems, representing the many-body Schrödinger equation as a set of coupled one-dimensional differential equations. Efficiency of the method has been repeatedly demonstrated by numerous investigations of few-body problems. Besides, this method has been constantly advanced by creating a more reliable and universal technique for description of the discrete and continuous spectra of many-body systems.

One of the direction for the HH method development is to use a full set of oscillator functions which are labelled by quantum numbers of the hyperspherical harmonics method. We will call them hyperspherical oscillator functions.

In the present paper, we study different channels of decay of three-cluster systems and ability of the hyperspherical oscillator functions to describe democratic and nondemocratic decay channels. In literature (see, for instance, Refs. [1–3]) a democratic decay is a synonym for three-body decay or full disintegration of a three-body system. This type of the decay is also called a “true” [4] or “truly” [5] three–body scattering. Contrary to the democratic decay, a non-

democratic decay stands for a decay of compound system into two fragments provided that one of the fragments is represented by a bound state of a two-body subsystem. In what follows we will consider only the dominant three-body configurations of light atomic nuclei.

Note that an oscillator basis is a conventional set of functions which are involved in many nuclear models, such as a traditional many-body shell model, the Resonating Group Method, novel ab initio No-Core Shell Model and many others.

Let us consider the following nuclei and appropriate (dominant) three-cluster configurations, as well as binary decay channels

$$\begin{aligned} {}^4\mathrm{He} &= d + p + n = {}^3\mathrm{H} + p = {}^3\mathrm{H}e + n = d + d\,, \\ {}^7\mathrm{Li} &= \alpha + d + n = {}^3\mathrm{He} + \alpha = {}^6\mathrm{Li} + n\,, \\ {}^8\mathrm{Be} &= \alpha + t + p = \alpha + \alpha = {}^7\mathrm{Li} + n\,, \\ {}^{10}\mathrm{Be} &= \alpha + \alpha + {}^2n = {}^6\mathrm{He} + \alpha = {}^8\mathrm{Be} + {}^2n, \end{aligned} \tag{1}$$

Here we indicated only those two-cluster decay channels of the three-cluster systems which have a bound state in the corresponding two-cluster subsystem. In other words, we disregard those binary channels whose threshold energy exceed the three-cluster threshold.

We are going to study the eigenspectrum of a microscopic hamiltonian of the above-mentioned three-cluster systems. For this aim we will construct matrix elements of the hamiltonian between many-particle cluster oscillator functions. Diagonalization of the matrix yields eigenvalues and the corresponding eigenfunctions. Some of the obtained eigenvalues represent bound states of the compound system, however the largest part of the eigenvalues are discretized states in two- or three-cluster continuum. The number of the eigenvalues and their density in the energy range in question depend on the number of oscillator functions involved in calculation and naturally on the properties of nucleus under consideration.

2 Method

We start model formulation with an explicit form of wave function for a system consisting of three s-clusters

$$\Psi_{LM_L} = \widehat{\mathcal{A}}\left\{\Phi_1\left(A_1\right)\Phi_2\left(A_2\right)\Phi_3\left(A_3\right)\psi_{LM_L}\left(\mathbf{x},\mathbf{y}\right)\right\}. \tag{2}$$

This is a traditional form of a wave function of the resonating group method for systems, when at least one cluster consists of two and more nucleons. The internal structure of clusters ($\alpha = 1, 2, 3$) is described by the antisymmetric and translationally invariant wave functions $\Phi_\alpha(A_\alpha)$. Function $\Phi_\alpha(A_\alpha)$ is a wave function of the many-particle shell model with the most compact configuration of nucleons. The antisymmetrization operator $\widehat{\mathcal{A}}$ makes antisymmetric the wave

function of the compound three-cluster system, which is of paramount importance for the energy region under consideration. Since all functions $\Phi_\alpha(A_\alpha)$ are fixed, to calculate a spectrum and wave functions of the compound system one has to determine a wave function of intercluster motion $\psi_{LM_L}(\mathbf{x},\mathbf{y})$. This function depends on two Jacobi vectors $\mathbf{x}$ and $\mathbf{y}$, locating relative position of clusters in the space. By using angular orbital momentum reduction, we represent this function as an infinite series

$$\psi_{LM_L}(\mathbf{x},\mathbf{y}) \Rightarrow \sum_{\lambda,l} \psi_{\lambda,l;L}(x,y) \left\{ Y_\lambda(\widehat{\mathbf{x}})\, Y_l(\widehat{\mathbf{y}}) \right\}_{LM_L}, \tag{3}$$

where $\widehat{\mathbf{x}}$ and $\widehat{\mathbf{y}}$ are unit vectors, and λ and l are the partial angular momenta associated with vectors $\mathbf{x}$ and $\mathbf{y}$, respectively.

Wave functions of intercluster motion $\psi_{\lambda,l;L}(x,y)$ obey an infinite set of the two dimension (in terms of variables x and y) integro-differential equations. To solve this equation we make use of the hyperspherical coordinates and hyperspherical harmonics. There are several schemes for introducing hyperspherical coordinates. We employ the hyperspherical harmonics in the form suggested by Zernike and Brinkman in Ref. [6], because this form is very simple, it does not involve bulky calculations and quantum numbers have clear physical meaning. To introduce the Zernike–Brinkman hyperspherical harmonics, we need to determine the hyperspherical coordinates. Instead of six variables $\mathbf{x}$ and $\mathbf{y}$ we introduce a hyperspherical radius and a hyperspherical angle

$$\rho = \sqrt{x^2+y^2}, \quad \theta = \arctan\left(\frac{x}{y}\right). \tag{4}$$

At a given value of ρ, the angle θ determines relative length of the vectors $\mathbf{x}$ and $\mathbf{y}$

$$x = \rho\cos\theta, \quad y = \rho\sin\theta, \quad \theta \in [0,\pi/2]. \tag{5}$$

In new coordinates

$$\Psi_{LM_L} = \sum_{K,\lambda,l} \widehat{\mathcal{A}} \left\{ \Phi_1(A_1)\, \Phi_2(A_2)\, \Phi_3(A_3)\, \phi_c(\rho)\, \mathcal{Y}_c(\Omega_5) \right\}, \tag{6}$$

where $\mathcal{Y}_c(\Omega_5)$ stands for the product

$$\mathcal{Y}_c(\Omega_5) = \chi_K^{(\lambda,l)}(\theta) \left\{ Y_\lambda(\widehat{\mathbf{x}})\, Y_l(\widehat{\mathbf{y}}) \right\}_{LM_L} \tag{7}$$

and represents a hyperspherical harmonic for a three-cluster channel

$$c = \{K,\lambda,l,L\}. \tag{8}$$

Definition of all components of the hyperspherical harmonic $Y_c(\Omega_5)$ can be found, for instance, in Ref. [7]. Being a complete basis, the hyperspherical harmonics account for any shape of the three-cluster triangle and its orientation.

They also account for all possible modes of relative motion of three interacting clusters.

As for the hyperradial wave functions $\phi_c(\rho)$, they obey a system of differential equations with local effective potentials for three structureless particles, or a set of integro-differential equations with nonlocal effective potentials for three clusters. To simplify solving a set of integro-differential equations, we invoke a full set of cluster oscillator functions to expand the sought wave function

$$\Psi_{LM_L} = \sum_{n_\rho, c} C_{n_\rho, c} \left| n_\rho, c \right\rangle .$$

This reduces a set of integro-differential equations to an algebraic form, i.e. to the system of linear algebraic equations

$$\sum_{\widetilde{n}_\rho, \widetilde{c}} \left[\left\langle n_\rho, c \left| \widehat{H} \right| \widetilde{n}_\rho, \widetilde{c} \right\rangle - E \left\langle n_\rho, c | \widetilde{n}_\rho, \widetilde{c} \right\rangle \right] C_{\widetilde{n}_\rho, \widetilde{c}} = 0. \tag{9}$$

Cluster oscillator functions for three-cluster configuration are determined as

$$\begin{aligned} \left| n_\rho, c \right\rangle &= \left| n_\rho, K; \lambda, l; L \right\rangle \\ &= \widehat{\mathcal{A}} \left\{ \Phi_1(A_1) \Phi_2(A_2) \Phi_3(A_3) R_{n_\rho K}(\rho, b) \mathcal{Y}_c(\Omega_5) \right\}, \end{aligned} \tag{10}$$

where $R_{n_\rho, K}(\rho, b)$ is an oscillator function (see definition in Ref. [7]) and b is an oscillator length.

System of equations (9) can be solved numerically by imposing restrictions on the number of hyperradial excitations n_ρ and on the number of hyperspherical channels c_1, c_2, …, $c_{N_{ch}}$. The diagonalization procedure may be used to determine energies and wave functions of the bound states. However, the proper boundary conditions have to be implemented to calculate elements of the scattering S-matrix and corresponding functions of continuous spectrum.

Wave function (10) belongs to the oscillator shell with the number of oscillator quanta $N_{os} = 2n_\rho + K$. It is convenient to numerate the oscillator shells by N_{sh} (= 0, 1, 2, …), which we determine as $N_{os} = 2n_\rho + K = 2N_{sh} + K_{\min}$, where $K_{\min} = L$ for normal parity states $\pi = (-1)^L$ and $K_{\min} = L + 1$ for abnormal parity states $\pi = (-1)^{L+1}$.

3 Results and Discussion

We involve the Minnesota potential (MP) [8] as a nucleon-nucleon potential in our calculations. We use a common oscillator length for all clusters. Its value is selected to minimize the energy of three-cluster threshold. To construct a wave function of two-cluster relative motion and to determine the energy of a two-cluster bound state, we employ oscillator basis. Details of two-cluster calculations can be found in Ref. [9]. We make use of 50 oscillator functions to calculate the ground state energies of two-cluster systems. This number of

Table 1. Input parameters of calculations for each nucleus.

Nucleus	3C-config.	b, fm	u
^{7}Li	$\alpha + d + n$	1.311	0.9255
^{7}Be	$\alpha + d + p$	1.311	0.9255
^{8}Be	$\alpha + {}^3H + p$	1.311	0.9560
^{10}Be	$\alpha + \alpha + {}^2n$	1.356	0.9570

functions provides correct value of bound state energies and their parameters (for instance, r.m.s. proton and mass radii and so on).

In Table 1 we show input parameters of our calculations. It includes oscillator length b and exchange parameters u of the selected NN potential.

Consider evolution of ^{7}Li spectrum when we involve more and more hyperspherical harmonics. We consider the $3/2^-$ state in both nuclei. This state is mainly represented by the total orbital momentum $L = 1$. We restrict ourselves by the only value of the total spin $S = 1/2$, and neglect contribution of negative parity state with total orbital momentum $L = 2$. For the total orbital momentum $L = 1$, we have only odd values of the hypermomentum $K = 1, 3, 5\ldots$. Thus we represent results with $K = 1$, $K = 3$ and so on up to $K_{\max} = 13$.

Dependence of energy of the $3/2^-$ states in ^{7}Li on quantum number N_{sh} is displayed in Figure 1. Here we presented trajectories of eigenvalues for ^{7}Li calculated with the hyperspherical harmonics $K_{\max} = 7$, $K_{\max} = 9$, $K_{\max} = 11$ and $K_{\max} = 13$. Figure 1 demonstrates rather fast convergence of the ^{7}Li

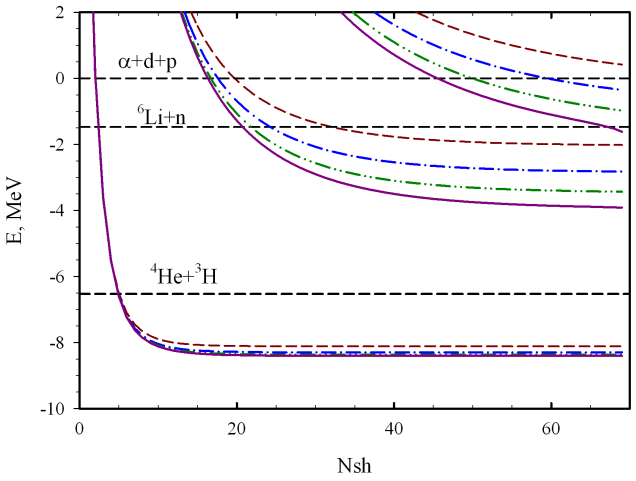

Figure 1. Spectrum of the $3/2^-$ states in ^{7}Li as a function of N_{sh} and $K_{\max}$. Dashed line – $K_{\max} = 7$, dot-dashed line – $K_{\max} = 9$, dot-dot-dashed line – $K_{\max} = 11$ and solid line – $K_{\max} = 13$.

ground state energy. For the sake of convenience in Figure 1 we connected all discrete points by lines, however the results are relevant only for discrete values of N_{sh}. Thus we need only restricted number of the hyperspherical harmonics ($K_{\max} = 7$) and small number of hyperradial excitations (or oscillator shells $N_{sh} \leq 30$) to obtain the bound state in ^{7}Li, i.e. an eigenstate of three-cluster compound system which lies below the lowest two-cluster threshold ^{4}He+^{3}H. The first eigenvalue for all values of $K_{\max}$ "scans" two-cluster continuous spectrum with small values of N_{sh} ($\leq$5) and thus represents continuous spectrum states in the ^{6}Li+n channel and in the ^{4}He+^{3}H channel. The second eigenvalue of the three-cluster hamiltonian for $7 \leq K_{\max} \leq 13$ is able to describe continuous spectrum states in three-cluster continuum and in binary channels continuum. The larger is the number of the hyperspherical harmonics involved in calculations, the larger region of two-cluster ^{4}He+^{3}H continuum can be achieved with these basis functions.

In Table 2 we present average distances between clusters in ^{7}Li ground and excited 3/2$^-$ states, calculated with $K_{\max} = 13$. These quantities determine the most probable shape of a triangle joining the centers of mass of interacting clusters. How to calculate the average distances is explained in Refs. [10, 11]. For each tree, R_2 stands for the average distance between a pair of clusters indicated in brackets, and R_1 determines mean distance between the first cluster and the center of mass of the two-cluster subsystem. One can see that the ground state is a compact state in all threes of the Jacobi coordinates. The first excited state, as expected, has dominant ^{4}He+^{3}H structure, since ^{3}H nuclei as a binary subsystem $^3\text{H} = n + d$ is very compact and is located far away (8.13 fm) from ^{4}He. Quite similar structure is observed for the second excited state. This state, as one can see in Figure 1, lies below the n+^{6}Li threshold. In this state, the size of ^{3}H is slightly increased to 4.19 fm compared to the ground and the first excited states, and distance between ^{3}H and ^{4}He exceeds 9 fm. The third excited state is of different nature. It is located between two-cluster (n+^{6}Li) and the three-cluster thresholds, and thus has very distinguished two-cluster n+^{6}Li structure. Indeed,

Table 2. Average distances between clusters for the ground and excited $3/2^-$ states in ^{7}Li.

Tree	$\alpha + (n + d)$		$n + (d + \alpha)$	
E, MeV	R_1	R_2	R_1	R_2
-8.688	2.88	2.46	2.70	2.99
$E_{th}\left(^3H + \alpha\right)$=-6.654				
-3.939	8.13	3.12	5.81	8.03
-1.644	9.68	4.19	6.69	9.19
$E_{th}\left(n +^6 Li\right)$=-1.475				
-0.439	6.85	18.06	17.38	4.42
1.263	8.80	10.20	16.05	4.71

in this state the spacing between clusters d and ^{4}He, comprising ^{6}Li, is 4.42 fm, slightly more than in the ground state (≈3 fm); and the distance from neutron to the center of mass ^{6}Li is very large – more than 17 fm. It is important to recall that the first, second and other excited states belong to two- or three-cluster continua. The wave functions of these states, as was pointed out earlier, are normalized to unity within the selected size of a "discrete box". Thus, Table 2 presents not absolute values of intercluster distances, but their relative values.

Concluding this section we note that we have carried out similar investigations for a mirror nucleus ^{7}Be as three-cluster configuration $^7\text{Be} = \alpha + d + p$. The Coulomb interaction, which is more stronger in ^{7}Be, slightly changes energy of the two-cluster threshold ^{4}He+^{3}He and reduces the energy of the ^{7}Be ground state with respect to two- and three-cluster thresholds. Therefore, all results and conclusions deduced for ^{7}Li nucleus are valued for the mirror nucleus. For the lack of room in the present paper, we will not dwell on the results for ^{7}Be.

Now we consider spectrum of the 0^+ states in ^{8}Be. With the three-cluster configuration ^{4}He+^{3}H+p we have got the following binary channels: ^{4}He+^{4}He and ^{7}Li+p. We do not consider the binary channel ^{5}Li+^{3}H as its threshold energy exceeds the three-cluster threshold. The energy of 0^+ states in ^{8}Be, calculated with only one hyperspherical harmonic $K = 0$ and with $K_{\max} = 14$, as a function of N_{sh} is displayed in Figure 2. The first and important result is that only one hyperspherical harmonic ($K = 0$) is able to produce one state in the ^{4}He+^{4}He continuum and one state above the ^{7}Li+p threshold but below the three-cluster ^{4}He+^{3}H+p threshold. Besides, the "ground" 0^+ state appears in the two-cluster ^{4}He+^{4}He continuum starting with $N_{sh} = 2$, while the first excited state needs more than $N_{sh} = 30$ oscillator shells to appear in the ^{7}Li+p continuum. It is interesting to note (see the lower part of Figure 2), that hyperspherical harmonics with $K_{\max} = 14$ generate one bound state (below the ^{4}He+^{4}He threshold) and four states in two-cluster ^{4}He+^{4}He continuum and also two states in the ^{7}Li+p continuum. Thus this number of hyperspherical harmonics (i.e. all harmonics with $0 \leq K \leq 14$ or 36 channels) is able to describe some states of elastic ^{4}He+^{4}He and ^{7}Li+p scattering and the reaction ^{4}He+^{4}He $\Longleftrightarrow$ ^{7}Li+p at two discrete energy points. It should be stressed that these results are obtained without imposing the boundary conditions.

Let us consider spectrum of ^{10}Be, provided that ^{10}Be is treated as a $\alpha+\alpha+^2n$ three-cluster configuration, and analyze what is the most probable geometry of this three-cluster structure. In Table 3 we show the ground and the first excited 0^+ states in ^{10}Be. The results are obtained with the MP. In Ref. [9] the exchange parameter u of the potential was selected so to reproduce the energy of the ^{10}Be ground state with respect to the binary threshold ^{6}He+α. We use the same value of this parameter. With this value of the parameter u we obtained the relative position of the threshold energies of the binary ^{6}He+α and $^8\text{Be} + {}^2n$ channels indicated in Table 3.

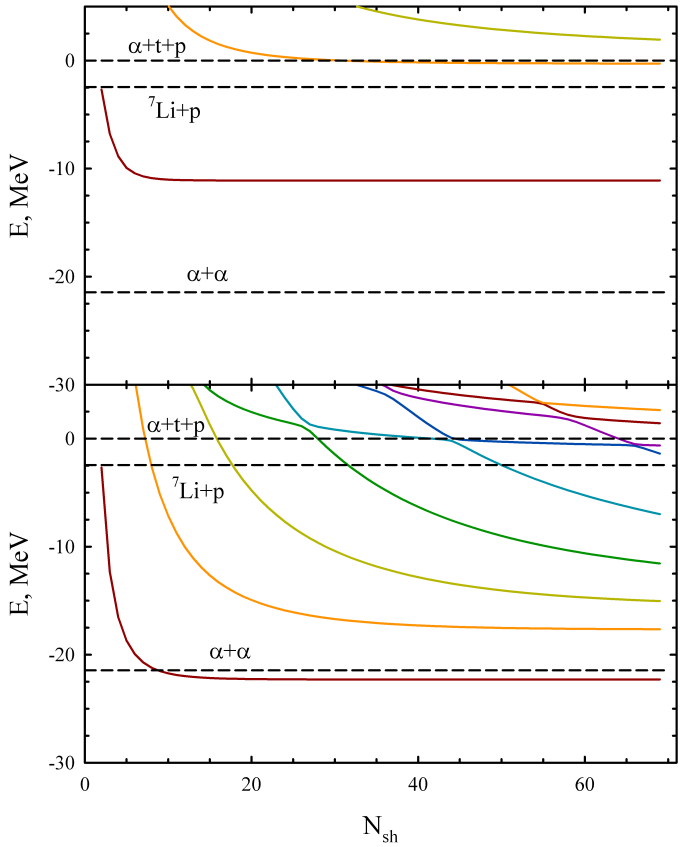

Figure 2. Spectrum of 0^+ states in ^{8}Be as a function of N_{sh}, calculated with $K_{\max} = 0$ (upper part) and $K_{\max} = 14$ (lower part of the figure).

Table 3. Energies (in MeV) of the ground and the lowest excited 0^+ states in ^{10}Be. Dominant two-body channels and their threshold energies E_{th} are also presented.

ν	0	1	2		3	4
E_ν	-9.16	-2.20	-0.34		0.56	1.16
E_{th}			-1.75	-0.02		
Channel			^{6}He+α	^{8}Be + ^2n		

As can be seen from Table 3, the ground state and the first excited 0^+ state are below the lowest binary decay threshold of ^{10}Be. The second excited state lies between ^{6}He+α and ^{8}Be + ^2n thresholds, while the rest of the states belong to three-cluster continuum.

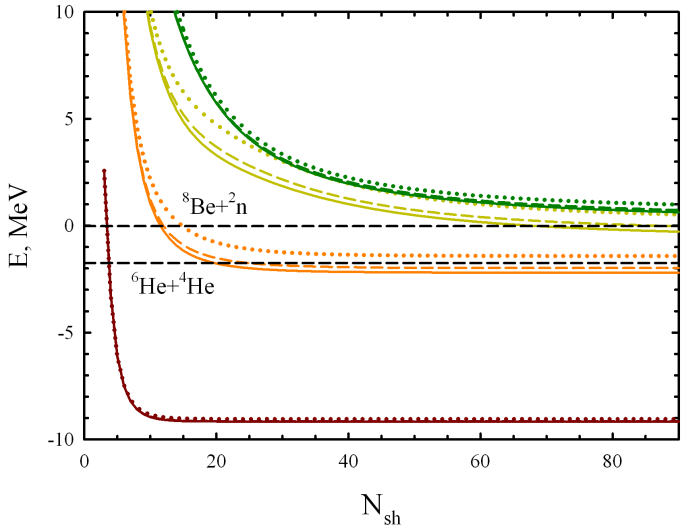

Figure 3. Spectrum of the 0^+ states in ^{10}Be as a function of N_{sh} and $K_{\max}$. Dotted lines correspond to $K_{\max} = 6$, dashed lines denote $K_{\max} = 10$, and solid lines stand for $K_{\max} = 14$.

Spectrum of the 0^+ states in ^{10}Be as a function of the number of oscillator shells and maximum value of hypermomentum involved in the calculations is plotted in Figure 3.

As evident from Figure 3, to reproduce the energy of the ground state it is sufficient to invoke basis functions with $N_{sh} = 20$ and $K_{\max} = 6$. The higher is the energy of the state, the larger value of the number of oscillator shells and hypermomentum should be used to reach the convergence. However, the third excited state with energy $E = 0.56$ MeV above the three-cluster decay threshold of ^{10}Be somewhat differs from the other states presented in Figure 3. Hyperharmonics with $K_{\max} \geq 10$ slightly contribute to the energy of this state as opposed to the neighbouring excited states.

4 Conclusion

Within a microscopic three-cluster model we have considered spectra of a set of light nuclei: ^{7}Li, ^{7}Be, ^{8}Be, ^{10}Be. We selected those nuclei which have a dominant three-cluster channel and one or more two-body channels below the three-cluster decay threshold.

The main result of the present investigations is that it is possible to see the evidence of two-cluster structure in the three-cluster wave function of a pseudo-bound state yet with a rather restricted set of the hyperspherical harmonics and hyperradial excitations as well. It was demonstrated that the eigenstates of the three-cluster hamiltonian have correct asymptotic behaviour both for bound

states below two-cluster threshold and states in two-cluster continuum. Analysis of the correlation functions in different Jacobi trees reveals polarizability of two-cluster bound states when the distance between the third cluster and two-cluster subsystem is relatively small.

References

[1] F. Aguila and M.G. Doncel, *Nuovo Cimento A* **59** (1980) 283-343.

[2] O.V. Bochkarev, L.V. Chulkov, A.A. Korsheninnikov, E.A. Kuz'min, I.G. Mukha, and G.B. Yankov, *Nucl. Phys. A* **505** (1989) 215-240.

[3] R.J. Charity, K. Mercurio, L.G. Sobotka, J.M. Elson, M. Famiano, A. Banu, C. Fu, L. Trache, and R.E. Tribble, *Phys. Rev. C* **75** (2007) 051304.

[4] R.I. Jibuti and R.Y. Keserashvili, *Czech. J. Phys.* **30** (1980) 1090-1100.

[5] E. Gerjuoy, *Phil. Trans. R. Soc. London A* **270** (1971) 197-287.

[6] F. Zernike and H. C. Brinkman, *Proc. Kon. Acad. Wetensch. Amsterdam* **38** (1935) 161-170.

[7] V. Vasilevsky, A.V. Nesterov, F. Arickx, and J. Broeckhove, *Phys. Rev. C* **63** (2001) 034606.

[8] D.R. Thompson, M LeMere, and Y.C. Tang, *Nucl. Phys. A* **286** (1977) 53-66.

[9] Yu.A. Lashko, G.F. Filippov, and V.S. Vasilevsky, *Nucl. Phys. A* **958** (2017) 78-100.

[10] V.S. Vasilevsky, *Ukr. J. Phys.*, **58** (2013) 544-553.

[11] A.V. Nesterov, V.S. Vasilevsky, and T.P. Kovalenko, *Phys. Atom. Nucl.* **77** (2014) 555-568.